Archives of Acoustics Vol. 47, No. 4, pp. 479–490 (2022), doi: 10.24425/aoa.2022.142900

Research Paper

Analysis of the Influencing Factors of the Acoustic Performance of the Muffler Considering Acoustic-structural Coupling

Bo ZHAO, He LI*

School of Mechanical Engineering and Automation, Northeastern University
Shenyang 110819, China

*Corresponding Author e-mail: hli@mail.neu.edu.cn

(*received June 21, 2022; accepted August 29, 2022*)

In the calculation of the acoustic performance of mufflers, the walls of mufflers are usually treated rigidly without considering the acoustic-structural coupling, but the results so calculated differ significantly from the actual situation. Based on the basic equations, the article derives the finite element equations of the muffler system while considering the acoustic-structural coupling effect and theoretically analyses the connection between the acoustic-structural coupling system and the structural and acoustic modes. The structural and acoustic modes of the muffler are calculated and the reasons for the mutation of the transmission loss curve of the muffler when the acoustic-structural coupling is considered are analysed. The results show that the acoustic-structural coupling is the result of the interaction between the structure and the air inside the expansion chamber under acoustic excitation, which manifests mutations in the sound pressure inside the muffler in some frequency bands. Then, using a single-chamber muffler as an example, the transmission loss is used to characterise the performance of the muffler. The effects of different factors such as shell thickness, structure, porous media material lining, and restraint method on the acoustic-structural coupling effect of the muffler are analysed, and the structure of a double-chamber muffler is successfully optimised according to the conclusions.

Keywords: acoustic performance; muffler; acoustic-structural coupling; transmission loss; mode; optimisation.

1. Introduction

In recent years, with the rapid development of industry and urbanisation, exhaust noise pollution has become an environmental pollution source that greatly affects people's lives in terms of health. At present, there are two main measures to control exhaust noise: one is to control the noise source, starting from the propagation mechanism of the noise source; the other is to install an exhaust muffler at the outlet of the exhaust, which is simple and effective, so it has become the most commonly used noise reduction method at home and abroad (Gupta *et al.*, 2018; Huang *et al.*, 2019; Ji, 2015)

In practice, the sound waves inside the muffler will excite the wall and cause the wall to vibrate, and the vibration will produce sound waves and at the same time the sound waves will excite the wall to vibrate. Therefore, the acoustic-structural coupling phenomenon exists in all cases, only the effect on the performance of the muffler is significant in some cases and negligible in others. In general, the acoustic-structural coupling phenomenon is more obvious for mufflers with larger structural dimensions and smaller rigidity. In this case, the acoustic-structural coupling effect of the muffler should not be ignored when calculating the acoustic performance of the muffler (Fan *et al.*, 2014). Considering the influence of acoustic-structural coupling in the calculation of muffler performance will make the calculation results more reliable and accurate. Research on the acoustic-structural coupling of mufflers has great significance for improving the design concept of mufflers and improving the reliability of the calculation of muffler acoustic characteristics.

Analytical methods of acoustic-structural coupling include analytical and numerical methods. The use of analytical methods to study the vibration and acoustic radiation of elastic structures began in the 1950s. The

analytical method is simple to use, has clear physical concepts, can reveal the nature of structural vibration and acoustic radiation, and is usually used to study structures with simple and regular shapes, such as flat plates, and spherical shells with axisymmetric properties, cylindrical shells, and others (Chen *et al.*, 2006). The finite element method is the main method used by researchers to investigate the coupling between vocal cavity and structure. Nefske *et al.* (1982) published several consecutive papers to study the interaction between structure and acoustics and to analyse the vibration and noise situation. Gladwell (1999; 2001) derived the energy equation for the coupling, considering the coupling effect for the first time, and Lyon (2005) proposed an acoustic-structural coupling model, providing the basis for the later studies. Yao *et al.* (2007) used the finite element method to calculate the acoustic modes inside the cavity and the vibration modes of the elastic plate along with their coupling coefficients. The above was combined with the boundary element method to calculate the sound pressure response outside the cavity and the results of this numerical simulation were compared with the analytical results derived earlier. Also, the correctness of the theoretical derivation was verified. Based on the acoustic finite element method and acoustic-structural coupling theory, Tian *et al.* (2007) established a finite element model of the box structure and used the finite element analysis software ANSYS to analyse the vibration and internal noise of the box structure for two cases with different thicknesses of wall plates and different positions of reinforcement treatment, and determined the influence law of the change of some structural parameters on the internal noise of the box. Han *et al.* (2009) analysed the acoustic-solid coupling of conical shell structures and compared them with experimental results, which showed that considering the coupling was closer to the actual situation. Li (2011) established a coupling model of elastic plate-shell-acoustic cavity structure, applied this model to analyse the acoustic-solid coupling characteristics of an elastic plate-cylindrical shell closed structure with one end fixed and one end closed, and verified the correctness of the model. Bai *et al.* (2011) studied the effect of acoustic-structural coupling on the dynamic characteristics of thin-walled cylindrical structures. Vijayasree, Munjal (2012) and Chiu (2013) used theoretical calculations and simulations to analyse the transmission loss of a complex muffler and verified the conclusions. Baruah and Chatterjee (2018) treated the muffler wall as elastic and carried out the modal analysis of the two mufflers, perforated and non-perforated, under static and dynamic loading, and the results showed that the modal vibration shapes of the two mufflers exhibited the same form of vibration at natural frequencies. To accurately predict the acoustic performance of water mufflers, Gong *et al.* (2018) used a two-dimensional axisymmetric model to analyse the internal sound field of the muffler using the acoustic-structural coupling model and calculated its transmission loss. Yokoyama (2021) has numerically simulated the vibration modes of the violin body to predict the characteristics of the vibration and sound radiation of the violin and analysed the sound radiation using the finite element method. The effects of the density and longitudinal stiffness of the violin material on its characteristic frequencies and sound radiation were analysed using the structural-acoustic coupling method. Fu *et al.* (2021) used the automatic matched layer (AML) technique to calculate the TL of the muffler under various design parameters, and compared and analyzed the influence law of several major parameters of the muffler on TL. It was found that the performance of the muffler was most obviously influenced by the length to diameter ratio, followed by the long and the short axis ratio and sieve separator perforation rate. It provided a theoretical basis for the design of the muffler parameters.

In summary, most of the previous studies on the sound-structure coupling phenomenon have focused on closed structures of specific volumes or indoor sound fields. The acoustic-structural coupling phenomenon is seldom considered in the calculation of the acoustic performance of mufflers, and few articles study the influencing factors that affect the acoustic-structural coupling of mufflers. Therefore, the research in this paper provides a reference basis for the design and structural optimisation of mufflers in the future and is of great significance.

2. Basic theory

2.1. Theory of acoustic-structural coupling

The acoustic-structural coupling method is based on the classical acoustic analysis method and solves the acoustic fluctuation equations of the system under certain boundary conditions. The main methods of acoustic-structural coupling analysis include analytical and numerical methods. Among them, the analytical method is limited to simple acoustic-structural coupling model solutions that cannot be applied to practical engineering problems. With the rapid development of numerical computing technology, the numerical method has been widely used in the analysis of coupled acoustic-structural systems.

Figure 1 shows a schematic diagram of the acoustic-structural coupling system. It consists of the structure domain Ω_s, the vocal cavity domain Ω_f, and the coupled interface Ω_{sf}. The boundary conditions of the domain include the displacement boundary condition Γ_u and the pressure boundary condition Γ_f.

The interaction between the acoustic waves and the structure occurs on the coupling interface between the solid structure of the muffler and the vocal cavity,

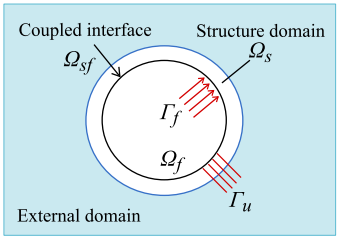

Fig. 1. Schematic diagram of the sound-structural coupling system.

and the acoustic pressure and displacement of the nodes on the coupling interface should be continuous, then the controlling equation of the acoustic-structural coupling boundary is as follows:

$$u_a \mathbf{n}_a = u_s \mathbf{n}_s, \tag{1}$$

where u_a is the displacement of the vocal cavity domain at the coupling boundary, u_s is the displacement of the structural domain at the coupling boundary, $\mathbf{n}_a$ is the normal vector of the surface of the vocal cavity at the coupling boundary, and $\mathbf{n}_s$ is the normal vector of the surface of the structure, and $\mathbf{n}_a = -\mathbf{n}_s$.

On the coupling interface of the acoustic-structural coupling system, the stress σ_s and sound pressure p on the interface of the structure have continuity, which is related as follows:

$$\sigma_s|_n = -p, \tag{2}$$

where $\sigma_s|_n$ is the normal projection of σ_s along with the interface of the structure.

When studying the coupling problem of sound and structure, it is necessary to establish the coupling equations of sound and structure. The air forms a cavity inside the muffler. Based on the basic acoustics equations, the finite element equations for the fluid medium inside the cavity are established:

$$[M_a]\{\ddot{P}\} + [C_a]\{\dot{P}\} + [K_a]\{P\} = \{F_a\}, \tag{3}$$

where $[M_a]$ is the fluid mass matrix, $[C_a]$ is the fluid damping matrix, $[K_a]$ is the fluid stiffness matrix, $\{P\}$ is the sound pressure vector at the unit node, and $\{F_a\}$ is the fluid load.

For elastic walls, the vibration of the muffler structure needs to be considered and its finite element equations are as follows:

$$[M_s]\{\ddot{U}\} + [C_s]\{\dot{U}\} + [K_s]\{U\} = \{F_s\}, \tag{4}$$

where $[M_s]$ is the structural mass matrix, $[C_s]$ is the structural damping matrix, $[K_s]$ is the structural stiffness matrix, $\{U\}$ is the displacement of the structural unit nodes, and $\{F_s\}$ represents the external excitation of the system.

When considering the coupling between the structure and the acoustic waves, the differential equations of the system need to take into account the effect of the coupling forces. The force of the acoustic pressure on the structure and the force of the structural motion on the vocal cavity are both set as additional external loads, and the differential equations of the structural and vocal cavity domains of the coupling system are expressed, respectively, as follows:

$$[M_s]\{\ddot{U}\} + [C_s]\{\dot{U}\} + [K_s]\{U\} = \{F_s\} + \{F_{as}\}, \tag{5}$$

$$[M_a]\{\ddot{P}\} + [C_a]\{\dot{P}\} + [K_a]\{P\} = \{F_a\} + \{F_{sa}\}. \tag{6}$$

Based on the continuity condition, assuming that the nodes of the structural domain on the coupling boundary correspond one-to-one to the nodes of the vocal cavity domain, the force $\{F_{as}\}$ applied to the coupling interface by the acoustic domain, and the force $\{F_{sa}\}$ applied to the coupling interface by the structural domain can be expressed as follows:

$$F_{as} = \int_{\Omega_{sf}} N_s^T P \mathbf{n}_a \,\mathrm{d}\Gamma = P \int_{\Omega_{sf}} N_s^T \mathbf{n}_a N_a \,\mathrm{d}\Gamma, \tag{7}$$

$$F_{sa} = -\rho \int_{\Omega_{sf}} N_a^T \ddot{u}_a \,\mathrm{d}\Gamma = -\rho \left(\int_{\Omega_{sf}} N_a^T \mathbf{n}_a N_s \,\mathrm{d}\Gamma \right) \ddot{u}, \tag{8}$$

where N_a is the finite element shape function in the vocal cavity domain, N_s is the finite element shape function in the structural domain, and Γ denotes the coupling boundary.

The acoustic-structural coupling matrix is denoted as $[R]$ and expressed as Eq. (9):

$$R = \int_{\Gamma_{sf}} N_s^T \mathbf{n}_a N_a \,\mathrm{d}\Gamma_{sf}, \tag{9}$$

Let us bring Eq. (9) into Eqs (7) and (8) for simplification:

$$F_{as} = RP, \tag{10}$$

$$F_{sa} = -\rho R^T \ddot{u}. \tag{11}$$

The finite element equations for the acoustic-structural coupling system are obtained by combining Eq. (5) to (11):

$$\begin{bmatrix} M_s & 0 \\ \rho R^T & M_a \end{bmatrix} \begin{Bmatrix} \ddot{U} \\ \ddot{P} \end{Bmatrix} + \begin{bmatrix} C_s & 0 \\ 0 & C_a \end{bmatrix} \begin{Bmatrix} \dot{U} \\ \dot{P} \end{Bmatrix} + \begin{bmatrix} K_s & -R \\ 0 & K_a \end{bmatrix} \begin{Bmatrix} U \\ P \end{Bmatrix} = \begin{Bmatrix} F_s \\ F_a \end{Bmatrix}. \tag{12}$$

Assuming that both the displacement and the acoustic wave are harmonic functions, Eq. (12) can be further expressed as follows:

$$\begin{bmatrix} K_s - \omega^2 M_s + j\omega C_s & -R \\ \rho\omega^2 R^T & K_a - \omega^2 M_a + j\omega C_a \end{bmatrix} \begin{Bmatrix} U \\ P \end{Bmatrix} = \begin{Bmatrix} F_s \\ F_a \end{Bmatrix}. \tag{13}$$

Equation (13) is a direct coupling method to solve the sound pressure and displacement of the acoustic-structural coupled system, but the coefficient matrix on the left side of the equation is an unsymmetrical matrix, which is computationally intensive and takes a long time to solve. To solve this problem, the modal superposition method is introduced, which forms the system response by superimposing the structural and acoustic modalities of the system:

$$\{U\} = \{\Phi_s\}\{X_s\}, \tag{14}$$

$$\{P\} = \{\Phi_a\}\{X_a\}, \tag{15}$$

where $\{\Phi_s\} = \{\Phi_{s1}, \Phi_{s2}, ..., \Phi_{sn}\}$ is the structural modal matrix in the absence of coupling, and $\{\Phi_a\} = \{\Phi_{a1}, \Phi_{a2}, ..., \Phi_{an}\}$ is the acoustic modal matrix in the absence of coupling, $\{X_s\}$ is the structural modal participation factor, and $\{X_a\}$ is the acoustic modal participation factor.

Let us bring Eqs (14) and (15) into Eqs (12) and (13):

$$\begin{bmatrix} m_s & 0 \\ \rho r^T & m_a \end{bmatrix}\begin{Bmatrix} \ddot{X}_s \\ \ddot{X}_a \end{Bmatrix} + \begin{bmatrix} c_s & 0 \\ 0 & c_a \end{bmatrix}\begin{Bmatrix} \dot{X}_s \\ \dot{X}_a \end{Bmatrix} + \begin{bmatrix} k_s & -r \\ 0 & k_a \end{bmatrix}\begin{Bmatrix} X_s \\ X_a \end{Bmatrix} = \begin{Bmatrix} f_s \\ f_a \end{Bmatrix}, \tag{16}$$

$$\begin{bmatrix} k_s - \omega^2 m_s + j\omega c_s & -r \\ \rho\omega^2 r^T & k_a - \omega^2 m_a + j\omega c_a \end{bmatrix}\begin{Bmatrix} X_s \\ X_a \end{Bmatrix} = \begin{Bmatrix} f_s \\ f_a \end{Bmatrix}, \tag{17}$$

where

$$\{m_s\} = \{\Phi_s\}^T [M_s]\{\Phi_s\}, \qquad \{c_s\} = \{\Phi_s\}^T [C_s]\{\Phi_s\},$$
$$\{k_s\} = \{\Phi_s\}^T [K_s]\{\Phi_s\}, \qquad \{f_s\} = \{\Phi_s\}^T [F_s],$$
$$\{m_a\} = \{\Phi_a\}^T [M_a]\{\Phi_a\}, \qquad \{c_a\} = \{\Phi_a\}^T [C_a]\{\Phi_a\},$$
$$\{k_a\} = \{\Phi_a\}^T [K_a]\{\Phi_a\}, \qquad \{f_a\} = \{\Phi_a\}^T [F_a],$$
$$\{r\} = \{\Phi_s\}^T [R]\{\Phi_a\}.$$

2.2. Modal analysis theory

As an inherent property of a system, each order of modal has its fixed frequency, vibration mode, damping, stiffness, and other parameters. There are two methods commonly used for modal analysis. One is the computational analytical method, which uses numerical analysis to obtain the eigenvalues and eigenvectors by solving the differential equations of the system, and the other is the experimental analytical method, which uses the input and output signals of the experimental measurement points to obtain the frequency and damping of the system, and then calculates the modal parameters. This paper mainly uses the computational analytical method to analyse the mode of the muffler.

The muffler structure system is a linear system with multiple degrees of freedom, and its oscillatory differential equation is generally expressed as Eq. (4). The external structural system of the muffler can be regarded as an undamped system, and under free vibration, the parameters $[C_s]$ and $\{F_s\}$ are both zero, then the undamped free vibration differential equation of the muffler structure can be expressed as follows:

$$[M_s]\{\ddot{U}\} + [K_s]\{U\} = 0. \tag{18}$$

Assuming that the vibration of the system can be decomposed as a superposition of a series of simple harmonic vibrations, the solution of Eq. (18) can be expressed as follows:

$$U = \varphi e^{i\omega t}, \tag{19}$$

where ω is the angular frequency of the simple harmonic vibration.

The characteristic equation of the muffler structure is obtained by combining Eq. (18) and Eq. (19):

$$\{\varphi_i\}\left([K_s] - \omega_s^2 [M_s]\right) = 0, \tag{20}$$

where ω_s is the angular frequency, and φ_i is the eigenvector, i.e. the amplitude vector; $s = 1, 2, 3, ..., n$.

The n eigenvectors and eigenvalues of the muffler structure can be obtained by calculating Eq. (20), which is the vibration mode and amplitude of the muffler structure.

The finite element matrix equation for the fluid in the expansion chamber of a muffler is generally expressed as Eq. (3). Neglecting the fluid damping $[C_a]$ and the externally applied load $\{F_a\}$, the differential equation for the fluid inside the muffler can be expressed as follows:

$$[M_a]\{\ddot{P}\} + [K_a]\{P\} = 0. \tag{21}$$

The characteristic equation of Eq. (21) can be expressed as follows:

$$\{p_j\}\left([K_a] - \omega_a^2 [M_a]\right) = 0. \tag{22}$$

The n eigenvectors and eigenvalues of the fluid medium inside the muffler can be obtained by calculating Eq. (22), which is the sound pressure mode and amplitude inside the muffler.

3. Acoustic-structural coupling analysis of the muffler

3.1. Modal analysis

To analyse the characteristics of the acoustic-structural coupling of the muffler more intuitively and clearly, a simple single-chamber exhaust muffler is selected as the object of study in this section, and its structural model and main parameters are shown in Fig. 2 and Table 1.

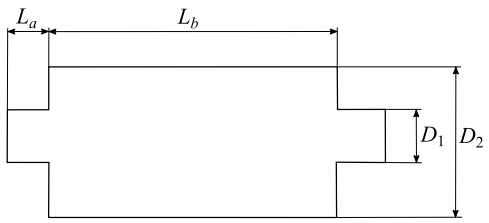

Fig. 2. Muffler structure diagram.

Table 1. Structural sizes of the muffler.

Parameter	Size [mm]
L_a	50
L_b	400
D_1	40
D_2	200

After establishing the structural model, the structural finite element analysis system and the acoustic finite element analysis system of the muffler are established. In the structural modal analysis, according to the actual installation of the muffler, one end of the inlet is set to be restrained, the outlet is set to be free, and the thickness of the shell is set to 1 mm. The material used for the muffler is structural steel whose density is 7850 kg/m^3, Young's modulus is $200 \cdot 10^9$ Pa, and Poisson's ratio is 0.30. The calculated partial modal frequencies and cloud images are shown in Table 2 and Fig. 3.

Table 2. Structural modal frequency value of the muffler.

Modal order	Frequency [Hz]
1	6.412
2	38.713
3	146.31
4	165.82
5	199.51
6	467.34
7	520.41
8	548.86
9	614.58
10	741.35

The muffler is filled with air, and the vocal cavity made up of the air also has its independent modes. The structural modal vibration is expressed as a change in the displacement of the muffler structure, while the acoustic mode of the vocal cavity is expressed as a change in the sound pressure inside the muffler. The partial acoustic mode frequencies of the muffler are shown in Table 3, and the partial modal vibration shapes are shown in Fig. 4.

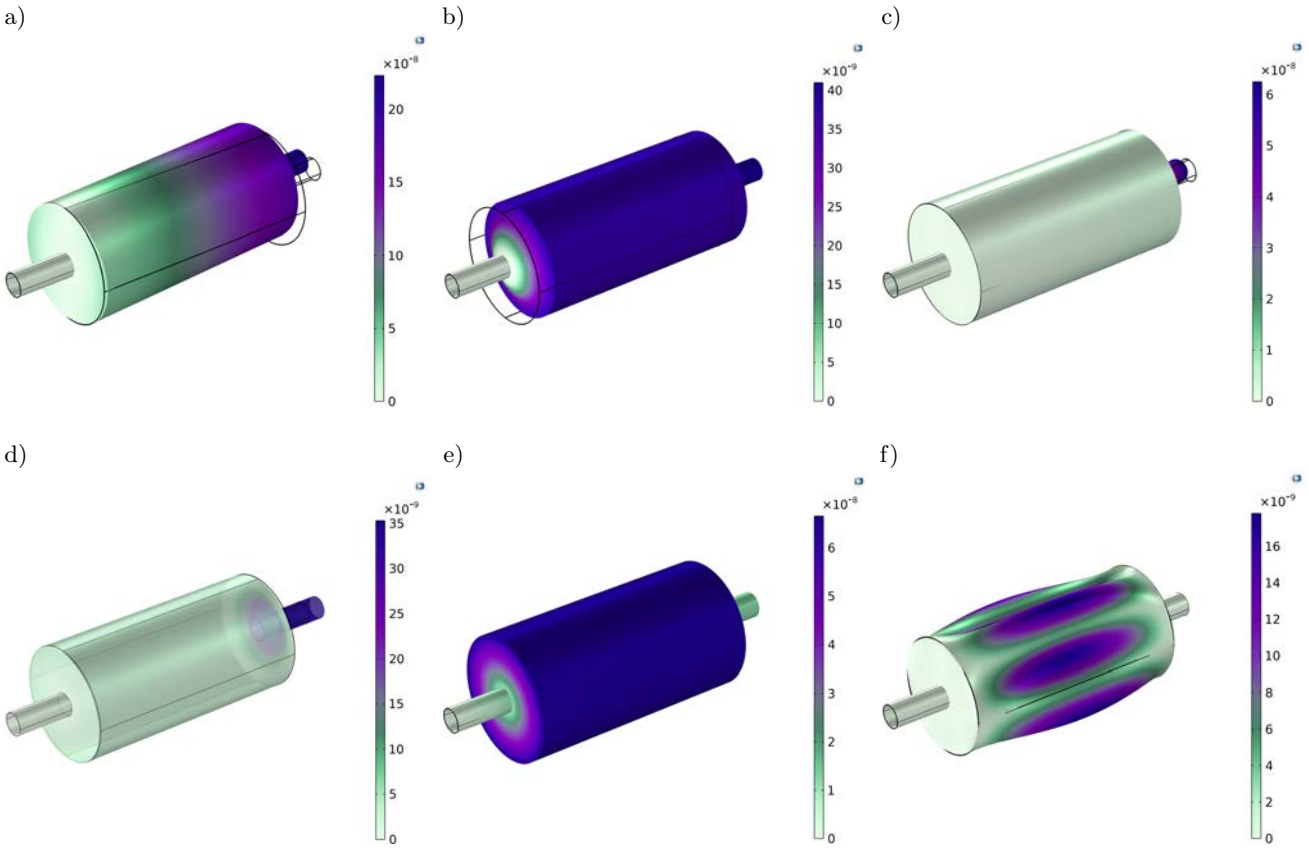

Fig. 3. Structural modal clouds of the muffler: a) first order, b) second order, c) third order, d) fourth order, e) fifth order, f) sixth order.

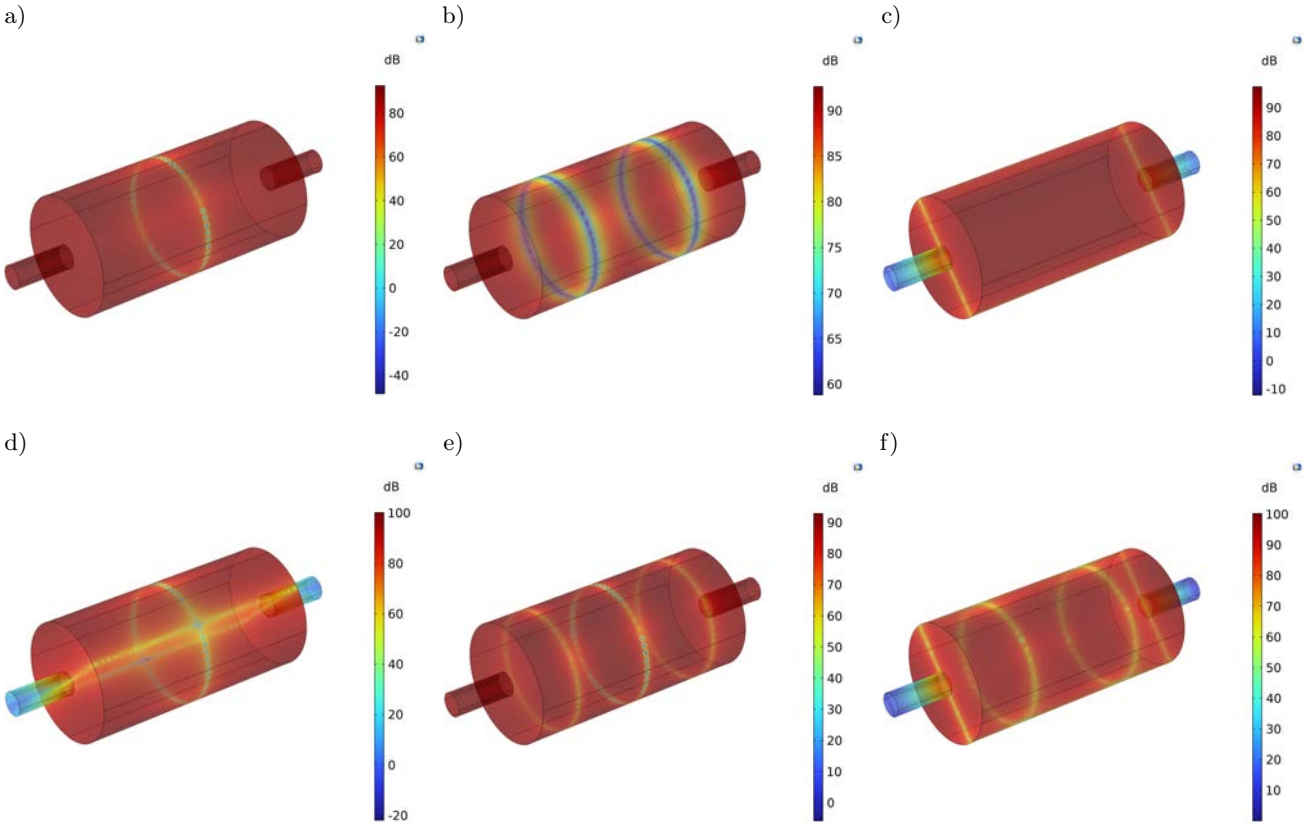

Fig. 4. Acoustic modal clouds of the muffler: a) first order, b) second order, c) third order, d) fourth order, e) fifth order, f) sixth order.

Table 3. Acoustic modal frequency value of the muffler.

Modal order	Frequency [Hz]
1	430.04
2	860.1
3	1006.9
4	1095.7
5	1290.2
6	1323.9
7	1634.9
8	1668.4
9	1722.8
10	1876.3

In summary, the modal frequencies and modal shapes of the structural and acoustic modes of the muffler are obtained after simulation calculations. The structural mode is an inherent and integral characteristic of an elastic structure. Through modal analysis, it is possible to clarify the frequency band in which the structure is susceptible and the characteristics of its main modal shapes in each order. The acoustic mode is formed by the interference and reflection of incident sound waves of different frequencies, which causes different sound pressure changes at different locations in the chamber. The changes in internal sound pressure caused by the sound wave transmission in the muffler will produce acoustic excitation, which will cause deformation in the structure of the muffler and affect the performance of the muffler in some frequency bands.

3.2. Calculation of transmission loss of muffler

Generally, when calculating the performance of a muffler, the wall is regarded as rigid and the effect of wall vibration is ignored, but this is not consistent with the actual working conditions of the muffler. To further investigate the effect of acoustic-structural coupling on muffler performance, the transmission loss when considering acoustic-structural coupling is calculated for the single-chamber muffler in Fig. 2.

In the calculation, we set the chamber medium as the air, the inlet and outlet boundaries were set as the plane wave radiation, the inlet sound pressure was set as 1 Pa, the sound velocity in the air equaled c_0 (343 m/s), and the air density was ρ_0 (1.225 kg/m^3), we set the solid structure material as the structural steel, and the thickness was 1 mm.

In the calculation, the solid structure of the muffler is set as a rigid wall and elastic wall in turn and the sound power of the inlet and outlet are extracted, then two transmission loss curves are calculated according to Eq. (23), as shown in Fig. 5:

$$\mathrm{TL} = 10\log\left(\frac{W_{\mathrm{in}}}{W_{\mathrm{out}}}\right), \tag{23}$$

where TL denotes the transmission loss of the muffler, W_{in} denotes the sound power at the inlet, and W_{out} denotes the sound power at the outlet.

In Fig. 5, the transmission loss curve considering the acoustic-structural coupling is compared with the transmission loss curve without considering the coupling, and it can be seen that the overall muffler band does not change due to the coupling, but there are mutations of amplitude at some frequency points. Comparing the results of the modal analysis, it is found that the frequencies where the mutation occurs are very close to the structural modal frequencies of the muffler, which indicates that the mutation of the muffler transmission loss curve is caused by the acoustic-structural coupling that excites the structural modes of the muffler. Table 4 shows the comparison between the frequencies of the mutation points of the muffler transmission loss curve and the frequencies of the structural modes.

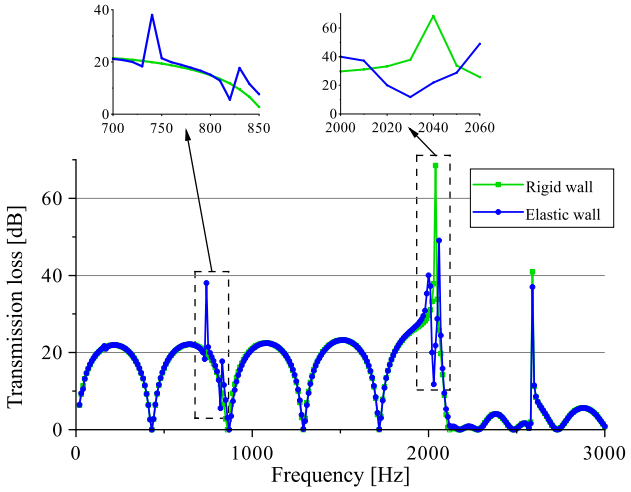

Fig. 5. Comparison of transmission loss curves.

Table 4. Comparison of curve mutation point frequencies and structural modal frequencies.

Frequency of curve mutation points [Hz]	Structural modal frequencies [Hz]
740	741.35
830	828.44
2030	2028.6

The curve that describes the coupling has two mutations in the 700–900 Hz band, with the amplitude of the transmission loss curve changing abruptly from 19.9 dB to 38.1 dB at 740 Hz, an increase of about 91.4%. In the 820–830 Hz band, there is a large fluctuation in the curve, with a transmission loss difference of about 12.2 dB from the valley to the peak. The largest mutation in the curve occurs at 2030 Hz, where the transmission loss decreases by 56.7 dB, a drop of about 82.8%. In the full frequency band, the average transmission loss with coupling is 13.05 dB, which is 0.91 dB less than the average transmission loss without coupling, a reduction of about 6.5%. In summary, although the overall average transmission loss of the muffler is not greatly reduced, the abrupt rise or fall of the noise reduction at some frequency points will still seriously affect the stability of the performance of the muffler. At the same time, the abrupt reduction of transmission loss in some frequency bands will cause problems such as squealing, which will affect the overall acoustic performance of the muffler.

4. Influencing factors of the acoustic-structural coupling

From the analysis in the previous section, it is clear that the muffler transmission loss curve will mutate when considering acoustic-structural coupling. In this section, the effect of different parameters such as shell thickness, structure, porous media material lining, and restraint method on the acoustic-structural coupling of the muffler are analysed and studied.

4.1. Shell thickness

Three different shell thicknesses of 1 mm, 1.5 mm, and 2 mm are set for mufflers of the same material (structural steel) to compare the effect of muffler acoustic-structural coupling for different shell thicknesses. As the shell thickness of the muffler changes, so does the structural modal. A comparison of the structural modal order frequencies for the three shell thickness mufflers is shown in Fig. 6.

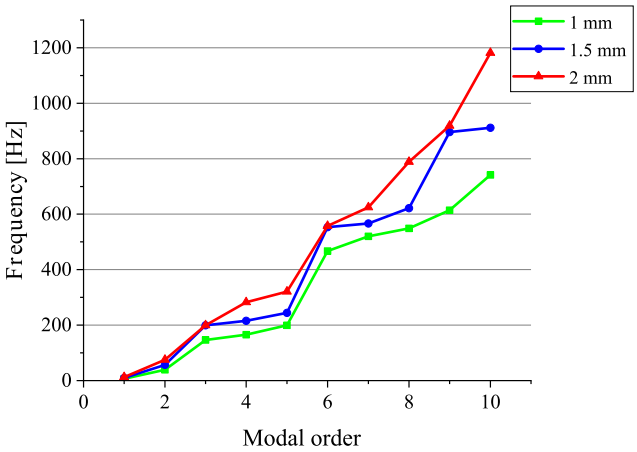

Fig. 6. Structural modal frequencies for mufflers of different thicknesses.

While comparing the structural modal frequencies of three different shell thickness mufflers, it was found that as the shell thickness of the muffler increases, the value of the structural modal frequency of the same order gradually increases. It indicates that as the shell

thickness of the muffler decreases, the structural mode becomes denser and is more likely to cause resonance. Based on the above modal analysis, the transmission loss calculation considering structure-acoustic coupling is carried out for mufflers with different shell thicknesses, and the calculation results are shown in Fig. 7.

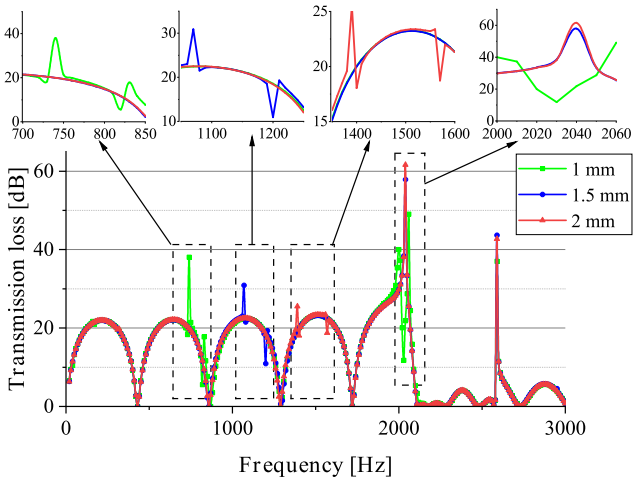

Fig. 7. Transmission loss curves for mufflers of different thicknesses.

In Fig. 7, there are three mutations in the transmission loss curve of the 1 mm shell thickness muffler, and two mutations in the transmission loss curve for each of the 1.5 mm and 2 mm shell thickness mufflers. The relationship between the frequencies of mutations in these curves and the structural modal frequencies of the corresponding mufflers is shown in Table 5.

Table 5. Curve mutation point frequencies and structural modal frequencies of mufflers with different shell thicknesses.

Shell thickness [mm]	Frequency of curve mutation points [Hz]	Structural modal frequencies [Hz]
1	740	741.35
	830	828.44
	2030	2028.6
1.5	1070	1081.2
	1200	1197.9
2	1390	1407.2
	1570	1580.1

According to Fig. 7 and Table 5, it can be seen that for mufflers with different shell thicknesses, due to the different inherent frequencies, the resonant frequencies under the same excitation are also different, which is reflected in the different numbers and frequencies of resonance peaks on the transmission loss curve. The transmission loss curve of mufflers with 1 mm shell thickness first undergoes mutation, the number of mutation points is the largest in the whole frequency band, and the change in amplitude at the time of mutation is also the largest. At the same time, the frequency of the first mutation of the transmission loss curve increases with the increase of the shell thickness, and the amplitude of the mutation decreases, which is consistent with the trend of the change of the structural modal frequency with the shell thickness in Fig. 6. It indicates that under the same structural and restraint conditions, the thinner the wall thickness of the muffler, the smaller the stiffness, the more likely it is to be excited to vibrate under the same acoustic energy, and the more likely its transmission loss curve will show mutations. As the thickness of the muffler shell increases, the stiffness of the structure becomes greater, the ability of the structure to resist deformation becomes stronger and the effect of acoustic-structural coupling becomes weaker.

4.2. Insert-pipe

Insert-pipe is one of the common structures used in the design of mufflers and has a good effect on improving the performance of mufflers. There are two types of insert-pipe structures: double insert-pipe structure and single insert-pipe structure. According to Sec. 3, the transmission loss curves of single-chamber mufflers with different insert-pipe structures considering the sound-structure coupling are calculated, as shown in Fig. 8.

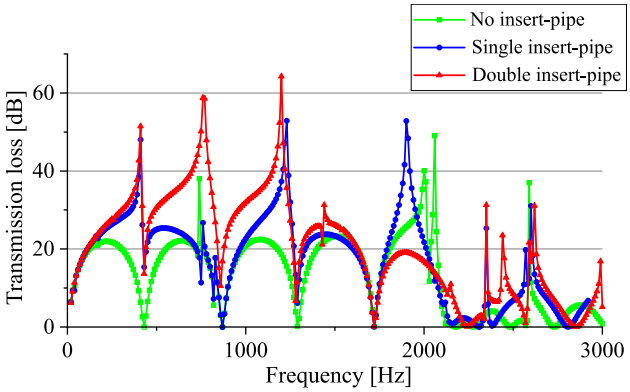

Fig. 8. Transmission loss curves of mufflers with different insert-pipe structures.

Figure 8 indicates that the performance of mufflers with different insert-pipe structures varies considerably. In general, the average transmission loss of the double insert-pipe muffler is 20.51 dB, which is better than that of the single insert-pipe muffler (17.56 dB) and the no-insert-pipe muffler (13.05 dB). In the 700–1000 Hz band, the curves of both single and no-insert-pipe mufflers mutate twice, while the curves of the double insert-pipe muffler do not mutate in this band. In the band 1700–2100 Hz, the performance of the single insert-pipe muffler is better than that of the double insert-pipe muffler. In summary, although the insert-

pipe structure can improve the overall performance of the muffler, the acoustic-structural coupling will cause mutations in the transmission loss curve of the muffler, which will result in the performance of the muffler and in some frequency bands being damaged. Therefore, when designing an insert-pipe muffler, the structure of the insert-pipe should be selected according to the distribution of the main noise frequencies of the target equipment.

4.3. Lining of the porous media material

The acoustic-structural coupling action occurs between the acoustic waves and the solid structure at the coupling interface. A layer of porous dielectric material with a flow resistivity of 1424.2 kg/(m^3·s) is laid on the interface surface. The transmission loss curves of a single-chamber muffler with a 1 mm and 2 mm porous media material layer are calculated, as shown in Fig. 9.

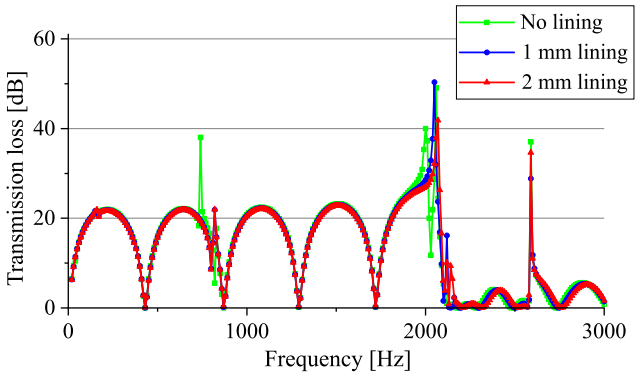

Fig. 9. Transmission loss curves of mufflers with different linings.

In Fig. 9, the transmission loss curve of the muffler with a layer of porous dielectric material is smoother than the curve without the lining. After the porous media material is applied, the mutation of the original curve (no lining) at 740 Hz and 2030 Hz disappears, the curve is smoother overall, and the performance of the muffler is improved.

4.4. Restraint methods

Considering the installation situation of the muffler, three categories are classified for different installation methods of the muffler. Class a is restraining the inlet orifice of the muffler, as shown in Fig. 10a; class b is restraining both the inlet and outlet of the muffler, as shown in Fig. 10b; and class c adds a set of restraints in the middle position of the chamber based on class b, as shown in Fig. 10c. The transmission losses of the muffler under different restraint conditions are calculated, and the relationship between the restraint method of the muffler and the acoustic-structural coupling is analysed.

Fig. 10. Installation categories of the muffler: a) class a, b) class b, c) class c.

The transmission loss curves of the muffler with different restraints are shown in Fig. 11. In general, the more restraints there are, the fewer the mutation points of the muffler transmission loss curve in the whole frequency band, the smaller the change in amplitude at the mutation, the smoother the curve, and the better the performance. After restraining the inlet and outlet ends simultaneously, the mutation at 830 Hz in the original curve (class a) disappears. The transmission loss in the frequency band around 2000 Hz of the muffler increases slightly with each additional set of restraints. In summary, an appropriate increase in restraint when installing a muffler will further limit the vibration of the muffler structure and inhibit mutations in certain frequencies. However, it is not the case that the more restrictions there are, the better the suppression effect. The type of restraint should be chosen on a case-by-case basis.

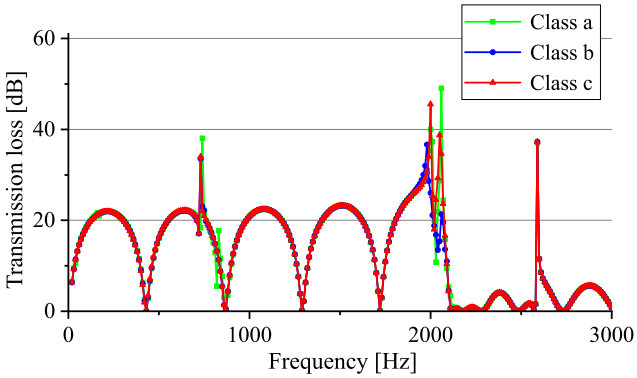

Fig. 11. Transmission loss curves of mufflers with different restraint methods.

5. Improvement of muffler performance considering acoustic-structural coupling

In the previous section, the influencing factors of acoustic-structural coupling have been analysed from four aspects. In this section, a double-chamber muffler matched with a dry vacuum pump is taken as the object of study, its performance is optimised according to the conclusions obtained in the previous section, and the basic structure and main parameters of this muffler are shown in Fig. 12 and Table 6.

According to the initial conditions in Sec. 3, the inlet of the muffler is restrained, the outlet is set to be free, and the material is set as structural steel. The

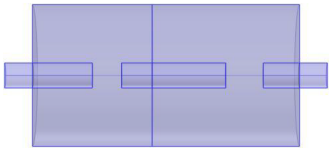

Fig. 12. Structure diagrams of the designed muffler.

Table 6. Parameter values of the muffler.

Parameter	Value [mm]
Total length	232
Lengths of each chamber	86–106
Length of each pipe	63–75–46
Diameter of chambers	102
Expansion ratio	5.66
Shell thickness	1.5

solid structure of the muffler is set in turn to be a rigid wall and elastic wall, and the transmission loss curves are calculated as shown in Fig. 13.

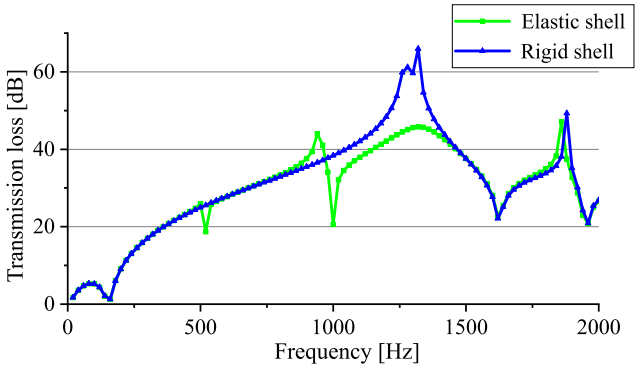

Fig. 13. Transmission loss curves of the double-chamber muffler.

In Fig. 13, the transmission loss curve of the double-chamber muffler mutates at 520 Hz, 940 Hz, and 1000 Hz when considering the effect of acoustic-structural coupling, while the transmission loss of the muffler decreases significantly in the 1000–1500 Hz frequency band. The average transmission loss in the full frequency range is reduced by 1.6 dB (about 6%), with the reduction of 20.2 dB (about 31%) occurring at 1320 Hz. Therefore, it is necessary to calculate and optimise the acoustic-structural coupling for the double-chamber muffler.

The structural modal analysis is carried out for the double-chamber muffler under the same initial conditions and the structural modal frequencies of the muffler within 2000 Hz are obtained, as shown in Table 7.

Table 7. Structural modal frequency value of the muffler.

Modal order	Frequency [Hz]
1	23.537
2	127.16
3	518.22
4	619.47
5	795.4
6	934.29
7	1008.3

The three frequencies where the curves in Fig. 13 mutate are all structural natural modal frequencies of the muffler, so in the process of optimizing the double-chamber muffler, consideration should first be given to how to avoid these modal frequencies being excited. Figure 14 shows the modal vibration shape of the double-chamber muffler at these natural modal frequencies.

In Fig. 14, the three modal vibration shapes of the double-chamber muffler are mainly excited at the central diaphragm and the outlet end baffle. Following the conclusions in Subsec. 4.4, keeping other conditions constant, the installation method of the double-chamber muffler is changed to restrain both the inlet and outlet ends, and the transmission loss curve of the muffler after increasing the restraint is calculated, as shown in Fig. 15.

As seen in Fig. 15, the mutation in the transmission loss curve at 520 Hz disappears after adding the restraint, indicating that the restraint at the outlet inhibits the outlet end baffle from being excited.

To further improve the performance of the double-chamber muffler, the structure of the double-chamber

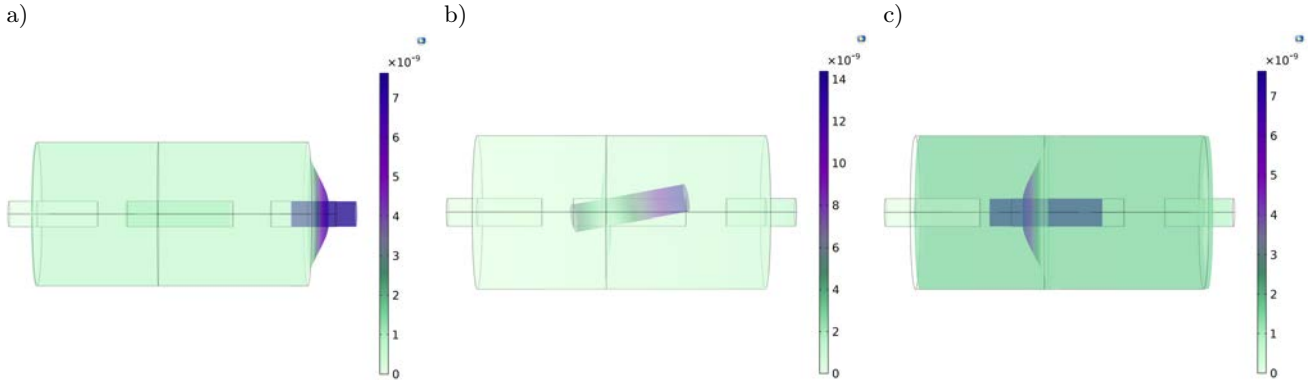

Fig. 14. Structural modal clouds of the double-chamber muffler: a) 518.22 Hz, b) 934.29 Hz, c) 1008.3 Hz.

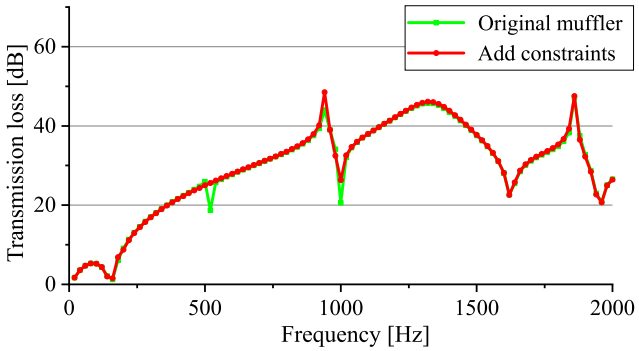

Fig. 15. Transmission loss curves of the double-chamber muffler with different restraint methods.

muffler is optimised following the conclusions obtained in Sec. 4. As seen in Fig. 14, the end cover and diaphragm of the double-chamber muffler are the parts that are susceptible to excitation, so the thickness of the end cover and diaphragm is increased from 1.5 mm to 3 mm, and then 2 mm of porous media material is laid on the inner surface of the chamber. The transmission loss curve of the optimised muffler is calculated and shown in Fig. 16.

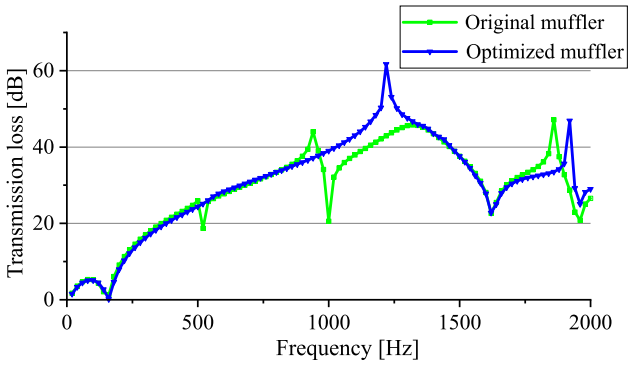

Fig. 16. Transmission loss curves of the optimised muffler.

As seen in Fig. 16, the transmission loss curve of the optimised muffler is smoother than that of the original muffler, and the number of mutations in the curve is significantly reduced. The average transmission loss of the muffler in the full frequency range is improved by 1.1 dB (about 4%), with the most significant improvement in the frequency range 950–1350 Hz, where the average transmission loss is increased by 6.5 dB (about 17%). Therefore, it can be concluded that the optimisation based on the conclusions in Sec. 4 is indeed effective in improving the acoustic performance of the muffler.

6. Conclusion

In this paper, based on previous research, the influence of muffler wall vibration is further considered comprehensively to improve the reliability of muffler acoustic performance calculation. The acoustic-structural coupling is negligible under general circumstances, but if the size of the muffler is larger or the stiffness is smaller, the excitation of the muffler wall by acoustic waves will become more and more obvious, and then the acoustic-structural coupling can no longer be neglected. The article takes a single-chamber muffler as the object of study, explores the acoustic performance of the muffler under the consideration of acoustic-structural coupling, analyses the influence of different parameters on the acoustic-structural coupling, and finally optimises a double-chamber muffler according to the conclusions. The main conclusions of this paper are as follows:

1) Acoustic-structural coupling is the result of the interaction between the muffler structure and the air in the expansion chambers under acoustic excitation, which is manifested as mutations in the transmission loss curve. The mutation caused by coupling is influenced by a certain order of acoustic mode or a certain order of structural mode. At the frequency of the mutation, the sound pressure and the amplitude of the structure inside the muffler will increase (or decrease) significantly compared to the adjacent points, affecting the stability of the performance of the muffler.
2) Transmission loss is used to characterise the performance of the muffler, and the effect of acoustic-structural coupling on the performance of the muffler is studied and analysed. The effects of different parameters such as muffler shell thickness, insert-pipe structure, porous media material lining, and restraint method on the acoustic-structural coupling effect of the muffler are analysed. The results show that increasing the shell thickness of the muffler, adopting the double insert-pipe, laying porous media material on the coupling interface, and increasing the restraint of the muffler can reduce the effect of acoustic-structural coupling and improve the performance of the muffler.
3) The conclusions in the single-chamber muffler were extended to the double-chamber muffler, and the transmission loss calculation and modal analysis are carried out for a double-chamber muffler taking into account the acoustic-structural coupling, and the weak parts of the double-chamber muffler are identified through the modal vibration shape, and the structure is optimised according to the conclusions from the single-chamber muffler. The results show that the acoustic performance of the optimised double-chamber muffler has improved significantly, with the average transmission loss of the muffler increasing by about 4% in the full frequency range, including an increase of about 17% in the 950–1350 Hz.

Acknowledgments

The study reported in this paper was financed by the National Natural Science Foundation of China, research project number 51675091.

References

1. Bai C., Zhou J., Yan G. (2011), Effects of sound field on thin-wall cylindrical structure dynamic characteristics, *Journal of Mechanical Engineering*, **47**(5): 78–84, http://qikan.cmes.org/jxgcxb/EN/Y2011/V47/I5/78.
2. Baruah S., Chattejee S. (2018), Structural analysis for exhaust gas flow through an elliptical chamber muffler under static and dynamic loading condition, *Advances in Modelling and Analysis B*, **61**(2): 92–98, doi: 10.18280/ama_b.610207.
3. Chen H., Mei-Ping S., Huanwen S. (2006), The numerical analysis of vibration and sound radiation efficiency from a cylindrical shell, *Noise and Vibration Control*, **8**(4): 51–54.
4. Chiu M.-C. (2013), Numerical assessment for a broadband and tuned noise using hybrid mufflers and a simulated annealing method, *Journal of Sound and Vibration*, **332**(12): 2923–2940, doi: 10.1016/j.jsv.2012.12.039.
5. Fan Z., Gui L., Ruiyi S.U. (2014), Research and development of automotive lightweight technology [in Chinese], *Journal of Automotive Safety and Energy*, **5**(01): 1–16, doi: 10.3969/j.issn.1674-8484.2014.01.001.
6. Fu J., Xu M., Zheng W., Zhang Z., He Y. (2021), Effects of structural parameters on transmission loss of diesel engine muffler and analysis of prominent structural parameters, *Applied Acoustics*, **173**: 107686, doi: 10.1016/j.apacoust.2020.107686.
7. Gladwell G.M.L. (1999), Inverse finite element vibration problems, *Journal of Sound and Vibration*, **221**(2): 309–324, doi: 10.1006/jsvi.1998.2011.
8. Gladwell G.M.L. (2001), On the reconstruction of a damped vibrating system from two complex spectra, Part 1: Theory, *Journal of Sound and Vibration*, **240**(2): 203–217, doi: 10.1006/jsvi.2000.3213.
9. Gong J., Xuan L., Zhou J., Peng C. (2018), Effects of acoustic solid interaction on acoustic characteristics of water expansion chamber muffler [in Chinese], *Journal of Harbin Institute of Technology*, **50**(10): 189–193, doi: 10.11918/j.issn.0367-6234.201712172.
10. Gupta A., Gupta A., Jain K., Gupta S. (2018), Noise pollution and impact on children health, *Indian Journal of Pediatrics*, **85**(4): 300–306, doi: 10.1007/s12098-017-2579-7.
11. Han F., Hu D-.K., Yan G.R. (2009), Vibration-acoustic coupling analysis of conical shell [in Chinese], *Noise and Vibration Control*, **29**: 30–33.
12. Huang H., Chen Z., Ji Z. (2019), One-way fluid-to-acoustic coupling approach for acoustic attenuation predictions of perforated silencers with non-uniform flow, *Advances in Mechanical Engineering*, **11**(5): 168781401984706, doi: 10.1177/1687814019847066.
13. Ji Z.L. (2015), *Acoustic Theory and Design of Muffler*, Beijing: Science Press.
14. Li Hongqiu (2011), *Acoustic vibration coupling analysis and optimization of vibration and noise reduction of plate/shell cavity structure* [in Chinese], Ph.D. Thesis, Nanjing University of Aeronautics and Astronautics.
15. Lyon R.H. (2005), Noise reduction of rectangular enclosures with one flexible wall, *The Journal of the Acoustical Society of America*, **35**(11): 1791–1797, doi: 10.1121/1.1918822.
16. Nefske D.J., Wolf J.A., Howell L.J. (1982), Structural-acoustic finite element analysis of the automobile passenger compartment: A review of current practice, *Journal of Sound and Vibration*, **80**(2): 247–266, doi: 10.1016/0022-460x(82)90194-8.
17. Tian H.L., Liu Z.F., Zhang N.L. (2007), Solid box on the acoustic coupling finite element analysis [in Chinese], *Machinery Design & Manufacture*, **07**: 24–26, doi: 10.3969/j.issn.1001-3997.2007.07.010.
18. Vijayasree N.K., Munjal M.L. (2012), On an Integrated Transfer Matrix method for multiply connected mufflers, *Journal of Sound and Vibration*, **331**(8): 1926–1938, doi: 10.1016/j.jsv.2011.12.003.
19. Yao H., Zhang J., Chen N., Sun Q.H. (2007), Analysis of sound radiation of elastic rectangular enclosure with considering boundary conditions [in Chinese], *Chinese Journal of Mechanical Engineering*, **43**(04): 163–167.
20. Yokoyama M. (2021), Coupled numerical simulations of the structure and acoustics of a violin body, *The Journal of the Acoustical Society of America*, **150**(3): 2058–2064, doi: 10.1121/10.0006387.